*sustainability*

MDPI

*Article*

# Compressive Shear Strength of Reinforced Concrete Walls at High Ductility Levels

**Tomislav Kišiček, Tvrtko Renić *, Damir Lazarević and Ivan Hafner**

Faculty of Civil Engineering, University of Zagreb, 10000 Zagreb, Croatia; tomislav.kisicek@grad.unizg.hr (T.K.); damir.lazarevic@grad.unizg.hr (D.L.); ivan.hafner@grad.unizg.hr (I.H.)

* Correspondence: tvrtko.renic@grad.unizg.hr

Received: 28 April 2020; Accepted: 27 May 2020; Published: 29 May 2020


**Abstract:** The amount of energy dissipated during an earthquake depends on the type of failure of the concrete element. Shear failure should be avoided because less energy is spent than that due to bending failure. Compression controlled failure is usually avoided by increasing the thickness of a wall. Considering that the current code largely decreases this strength, this becomes hard to achieve in practice. Because of that, the analysis described in this paper is made to determine the reason for a large strength reduction at high curvatures. Mechanisms contributing to compression controlled shear strength are analysed. Using Rankine's strength theorem, section equilibrium, arch mechanism and bending moment-curvature diagrams, the influence of different parameters are observed and charted. The findings are compared to the existing procedures and a new, simple and safe analytical equation is derived. Compression controlled shear strength is mainly influenced by axial force, followed by the amount of longitudinal reinforcement and the achieved confinement. Results show that the value of strength reduces significantly with the increase of ductility and that some reduction exists even for lower levels of curvature. Current code provisions may lead to unsafe design, so designers should be careful when dealing with potentially critical walls.

**Keywords:** analytical model; ductile walls; shear strength; capacity reduction; Eurocode 8

## 1. Introduction

Reinforced concrete walls are often used as elements for ensuring the lateral strength and stability of a structure. During an earthquake, a large amount of energy is released. In order for a structure to dissipate that energy, plastic deformations must occur and high ductility is necessary. To ensure a ductile behaviour, shear types of failure should be avoided and bending failure should precede it [1]. This is typical for reinforced concrete and masonry structures. Three types of shear failure are possible: due to diagonal tension (also called tension failure in this paper), due to diagonal compression (also called compression failure in this paper) and due to sliding [2]. They are presented in Figure 1.

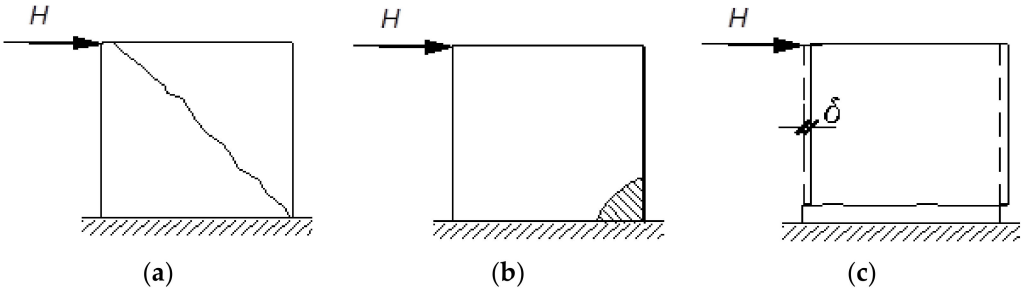


**Figure 1.** Shear failure: (**a**) tension controlled; (**b**) compression controlled; (**c**) sliding.

Both tension controlled and sliding failures can be avoided by adding reinforcement. In fact, the tension controlled strength of concrete is usually considered to be non-existent. Horizontal reinforcement is added to increase it. As for sliding, diagonal reinforcement may be added at the base of the wall. Compression controlled failure cannot be increased by any reinforcement according to the Eurocode for the design of new structures, EN 1998-1 [3]. According to the Eurocode for the assessment of existing structures, EN 1998-3 [4], reinforcement significantly increases strength—so much so that there is no upper limit to its influence. This discrepancy between the two parts of the same standard seems confusing, to say the least. European standards differentiate between three levels of ductility: low (DCL), medium (DCM) and high (DCH). Only the last two are applicable to buildings designed in seismic regions. According to [3], shear compressive strength for DCL and DCM can be determined with an equation given in Eurocode for the design of concrete structures, EN 1992-1-1 [5]. Buildings designed with DCH have a reduced value of compressive strength according to [3].

Experiments [6–8] show that reduction is also needed for DCM, but according to [9] it was not included in the code for new structures [3], so as not to limit the use of wall systems. It was included, however, in the code for existing structures [4]. The equation derived in [6] is purely empirical. It was later slightly modified in [8]. According to the *fib* Model Code 2010 [10], compressive shear strength is modified because of dynamic nature of the load, regardless of the required ductility level. Theoretical models of compressive shear strength reduction of columns have been explained in [11–18]. In addition to what was previously mentioned, experimental data on the shear strength of walls is given in [19–23], while analytical equations can be found in [24], but only for walls failing in bending or sliding.

In addition to the reduction of shear strength with higher ductility demand, shear demand increases because of the dynamic nature of the load. The reason for this is that during an earthquake shear force does not decrease as much as the bending moment (a smaller reduction/behaviour factor for shear than for bending should be implemented). This increase in demand is not correlated with the reduction of shear strength, so both should be considered when designing a structure. This usually means that a shear check is hard to carry out in practical structures. Only strength will be considered in this paper, but a detailed literature review about the dynamic increase of shear demand can be found elsewhere [25–28].

## 2. Methods of Determining Shear Strength

Four different methods will be analysed in this section—three from the existing codes and one based on the mechanical principles. The first three represent the currently used procedures, while the last one will be used to try and develop a new equation. Although some parts of this equation were proposed before [11–13], a unification of different mechanisms is presented in this paper. A parametric analysis was made and the influence of each parameter was analytically assessed. Some parameters that are usually not mentioned, like the reinforcement ratio or the ultimate curvature, are also discussed. Since analytical expressions are preferred to the empirical ones, and this mode of failure is critical, it is important to develop a simple unified equation with clear mechanisms.

### *2.1. EN 1998-1 Provisions*

Code EN 1998-1 [3] defines diagonal compressive strength in the same way as code EN 1992-1-1 [5], by an expression (Equation (1)):

$$V_{\mathrm{Rd}}{}^{\mathrm{EN\text{-}1}} = \alpha_{\mathrm{cw}} \times b_{\mathrm{w}} \times z \times \nu_1 \times f_{\mathrm{cd}}/(\cot\theta + \tan\theta), \quad (1)$$

where:

$\alpha_{\mathrm{cw}}$ coefficient of normal force influence,
$b_{\mathrm{w}}$ breadth of a wall,
$z$ internal lever arm (according to [3], it can be estimated as $z = 0.8 \times h$),
$h$ height of a wall cross section,

$\nu_1$ influence of cracks on strength $\nu_1 = 0.6 \times (1 - f_{ck}/250)$,
$f_{cd}$ design compressive strength of concrete and
$\theta$ compression strut angle (according to [3], the value of $\theta = 45°$ may be adopted).

The coefficient of normal force influence can have a value of $0 \leq \alpha_{cw} \leq 1.25$. For walls designed in accordance with [3], the coefficient can have a value of $1.0 \leq \alpha_{cw} \leq 1.25$. In other words, compressive force has a positive influence on shear strength. According to section 5.5.3.4.2 (1) (b) of code [3], compressive shear strength should be reduced to 40% of the value defined by Equation (1) when DCH is used, but no reduction is required if DCM (or DCL) is used. No clear direction is given as to what must be designed as DCH, which could lead to an engineer choosing a lower ductility class because it is less restrictive. This would mean a lower safety of a structure and should be avoided.

### *2.2. EN 1998-3 Provisions*

Code EN 1998-3 [4] defines diagonal compressive strength based on the experimental results summarized in [6–8]. The most recent paper, [8], proposes the following expression for shear strength (Equation (2)):

$$\tau_{Rd}{}^{EN\text{-}3} = 0.765 \times [1 - 0.06 \times \min(5; \mu_\theta{}^{pl})] \times [1 + 1.8 \times \min(0.15; N/(A_c \times f_c))] \times [1 + 0.25 \times \max(1.75; 100 \times \rho_{tot})] \times [1 - 0.2 \times \min(2; L_s/h)] \times \min(\sqrt{f_c}; 10\ \text{MPa}), \quad (2)$$

where:

$\mu_\theta{}^{pl}$ plastic rotation ductility factor $\mu_\theta{}^{pl} = \mu_\theta - 1$,
$\mu_\theta$ rotation ductility factor,
$N$ axial force,
$A_c$ cross section area of concrete,
$\rho_{tot}$ total vertical reinforcement ratio and
$L_s/h$ ratio of shear span to cross section height.

Equation (2) differs from the one given in [4] in some respects. Firstly, the constant 0.765 is substituted with 0.739 for primary seismic walls, and a shear force $V_{Rd}$ is given, rather than shear stress $\tau_{Rd}$. To obtain the shear force, $\tau_{Rd}$ should be multiplied by $b_w \times z$. It is obvious that the differences proposed in [8] and in [4] are not large. Since [8] is more recent and might be used in the new generation of codes, Equation (2) will be used in the rest of this paper. It is clear that Equations (1) and (2) have a completely different form, although both are used in the same collection of standards. Equation (2) is also dimensionally inconsistent, but many standards [29–31] propose dimensionally inconsistent equations. While (1) is developed from mechanical considerations, (2) is purely empirical.

In Equation (2), ductility is considered with a factor $\mu_\theta{}^{pl}$. Ductility may be expressed in a few different ways, most commonly with respect to deflection $\mu_\Delta$, rotation $\mu_\theta$ or curvature $\mu_\phi$. Rotation ductility is used in Equation (2), but curvature ductility will be used in the analytical analysis because it is easier to calculate the curvature ductility explicitly (but hard to measure). Although the curvature is denoted with 1/r in code [5], in this paper $\phi$ will be used. Ductility classes DCM and DCH differ only in the required ductility. The reduction of compressive shear strength with respect to ductility is given in Table 1. The reduction in Table 1 is defined only with respect to ductility, in other words only $(1 - 0.06 \times \min(5; \mu_\theta{}^{pl}))$ is calculated for different levels of ductility. Term reduction is used throughout this paper to denote the ratio of strength determined by a specific method and the strength determined using the Equation (1). Some mechanisms cause an increase of strength, but it will still be called reduction in this paper for the sake of expediency and the comparison of data.

**Table 1.** Influence of ductility on shear strength according to (2).

| $\mu_\theta{}^{pl}$ | Reduction |
|---|---|
| 0 | 1.00 |
| 1 | 0.94 |
| 2 | 0.88 |
| 3 | 0.82 |
| 4 | 0.76 |
| ≥5 | 0.70 |

It is clear from Table 1 that the increase in ductility continually decreases the shear strength, which is not in accordance with the proposal given in [3], where no reduction is used for DCM. Moreover, it is visible that ductility influences strength by 30% at most, unlike what is mentioned in code [3], where 60% reduction is proposed for DCH. Of course, different parameters might further reduce the strength, but that may happen regardless of the ductility class. Furthermore, it is not clear from Equation (2) how the cyclic and dynamic nature of the load influences the strength. It is mentioned in both [4] and [8] that the reduction is due to dynamic effects, but this is in no way apparent. Another thing that is not apparent from Equation (2) is which value of compressive strength should be used—mean or characteristic, confined or unconfined.

### 2.3. *Fib Model Code 2010 Provisions*

The *fib* model code [10] suggests the use of one of the three levels of precision to determine shear strength. The compression controlled failure in all of them is defined by an equation (Equation (3)):

$$V_{Rd}{}^{fib} = k_c \times f_{cd} \times b_w \times z \times \cot\theta/(1 + \cot^2\theta), \quad (3)$$

where: $k_c = 0.55 \times (30/f_{ck})^{1/3}$.

Equation (3) is used to determine the strength due to monotonic loads. For dynamic loads, Equation (3) should be reduced by an Equation (4) (reduction of strength):

$$\nu = 0.3 \times (1 - f_{ck}/250). \quad (4)$$

In Table 2, the reduction of shear strength is given with respect to concrete compressive strength.

**Table 2.** Reduction of cyclic compressive shear strength according to (4).

| Concrete Class | Reduction $\nu$ |
|---|---|
| C20/25 | 0.28 |
| C25/30 | 0.27 |
| C30/37 | 0.26 |
| C35/45 | 0.25 |
| C45/55 | 0.25 |
| C50/60 | 0.24 |

It is clear from Table 2 that the reduction is significantly larger according to the *fib* Model Code 2010 [10] than what is proposed in [3]. It is also important to notice that Equations (1) and (3) differ, so that reductions should not be compared directly. The important thing is that the reduction proposed by *fib* is not correlated with ductility, but only with the dynamic nature of the load. If this is the source of the reduction, why does EN 1998-1 differentiate between different ductility classes? Both the DCM and DCH structures experience a dynamic load during an earthquake. Another important thing to notice is that neither *fib* nor EN 1998-1 consider ductility explicitly.

### 2.4. Comparison of EN 1998-1 and EN 1998-3 Provisions

Compressive shear strength is calculated by Equations (1) and (2) and their comparison made for the high ductility class. DCH in [3] is not associated with a unique ductility, but rather depends on the system used, its geometry and simplicity. In this paper, a ductile wall system will be considered because the behaviour of such a system primarily depends on the behaviour of walls. For frame and coupled wall systems, the behaviour factor is usually larger. The behaviour factor for a DCH wall system is q ≥ 4.0.

The rotation ductility factor and curvature ductility are correlated to the behaviour factor by the Equation (5) used for $T_1 \geq T_C$:

$$\mu_\theta = q = 0.5 \times (\mu_\phi + 1), \quad (5)$$

where:

$T_1$ fundamental period of the structure in a given direction and
$T_C$ corner period dependent on the soil.

According to Equation (5), for DCH $\mu_\theta \geq 4.0$, ${\mu_\theta}^{pl} \geq 3.0$ and $\mu_\phi \geq 7.0$. In addition, if $T_1 < T_C$, the required ductilities increase. In the rest of the paper, if no ductility is explicitly mentioned, DCH will be considered to represent the ductility $\mu_\phi = 7$ (${\mu_\theta}^{pl} = 3.0$) and DCM to represent $\mu_\phi = 5$ (${\mu_\theta}^{pl} = 2.0$).

The minimum and maximum possible values of shear strength given by (2) are calculated for DCH walls (${\mu_\theta}^{pl} = 3.0$). Results are shown in Table 3. The maximum considered value of total vertical reinforcement ratio is $\rho_{tot} = 0.04$, and the maximum normalized axial force $N/(A_c \times f_c) = 0.35$ (those values correspond to the maximum values allowed in [3] for DCH). The minimum value of all factors is 0, except for $(L_s/h)_{min}$, which is equal to 1 (because experimental data did not include specimens with a lower ratio). Minimum and maximum values are then compared to the value calculated by (1). In Table 3, the values of shear strength calculated by Equation (1) are divided by $(b_w \times z)$ to be comparable to the values calculated by (2). The values $R_{min}$ and $R_{max}$ are the ratios of strength calculated by (2) (minimum or maximum) and by (1). In other words, they are reductions of strength. Table 3 shows that the variation of results is large (between the minimum and maximum possible value), regardless of the concrete used. Variation stays large even if only slender walls are considered (last column of Table 3).

**Table 3.** Minimum and maximum reduction of shear strength for high ductility.

| Concrete Class | ${\tau_{Rd,min}}^{EN-3}$ | ${\tau_{Rd,max}}^{EN-3}$ | ${V_{Rd,min}}^{EN-1}/(b_w \times z)$ | ${V_{Rd,max}}^{EN-1}/(b_w \times z)$ | $R_{min}$ | $R_{max}$ > $L_s/h = 1$ | $R_{max}$ $L_s/h \geq 1$ |
|---|---|---|---|---|---|---|---|
| C20/25 | 2.42 | 5.70 | 3.68 | 4.60 | 0.66 | 1.24 | 0.93 |
| C25/30 | 2.71 | 6.37 | 4.50 | 5.63 | 0.60 | 1.13 | 0.85 |
| C30/37 | 2.96 | 6.98 | 5.28 | 6.60 | 0.56 | 1.06 | 0.79 |
| C35/45 | 3.20 | 7.54 | 6.02 | 7.53 | 0.53 | 1.00 | 0.75 |
| C40/50 | 3.42 | 8.06 | 6.72 | 8.40 | 0.51 | 0.96 | 0.72 |
| C45/55 | 3.63 | 8.55 | 7.38 | 9.23 | 0.49 | 0.93 | 0.70 |
| C50/60 | 3.83 | 9.01 | 8.00 | 10,00 | 0.48 | 0.90 | 0.68 |

It is visible from Table 3 that the reduction of 0.4 given by code [3] is appropriate for a higher concrete class, low reinforcement ratio and low axial force ($R_{min}$). For a larger amount of reinforcement and a larger axial force, the reduction is smaller (the number in the table is closer to 1.00). For larger concrete classes, the reduction is larger. It is also important to notice that for a ductility higher than ${\mu_\theta}^{pl} = 3.0$, considered here, the reduction is larger (up to ${\mu_\theta}^{pl} = 5.0$).

### 2.5. Analytical Model of Compressive Shear Strength

Lateral forces cause shear forces and bending moments in walls. Due to bending moments, normal stresses occur in cross sections, and due to shear forces, shear stresses occur. The interaction of shear

and normal stresses can be substituted by principal tension and compression stresses at an angle. When the principal compressive stress reaches the compressive strength at a certain point, capacity is reached at that point. This principle is based on Rankine's maximum stress theory. Different theories may be used, but Rankine's theory was chosen in this paper because of its simplicity.

When the compressive strength of a material is known, it is possible to determine the residual shear capacity in any point for a given curvature of a section. The capacity of a whole section may be determined by the integration of shear capacities in each of the points along a compressed part of the section. Only the compressed part is considered, because after the yielding of reinforcement, the tension part of the section is considerably damaged due to cracking [11]. This consideration is conservative, since some of the tension part of a section probably also contributes to shear strength (an uncracked part near a neutral axis and a slightly cracked part next to it). Increasing the curvature of a section, normal stresses increase, leading to a reduction in shear capacity. According to this theory, strength reduction is not due to the dynamic nature of loading, but to the fact that a section is severely curved. In fact, since only section stresses are considered, compressive strength should increase with the increase of the strain rate (dynamic load), and with it shear strength. According to [10], a simplified method may be used to determine the influence of dynamic increase factors (DIF) depending on the type of check being made. No increase will be considered in this paper, since its influence is not large and would unnecessarily complicate the procedure.

According to Rankine's theory, shear capacity was determined in [32], following Equations (6) and (7) derived for failure due to compression:

$$\nu_{cc}(z) = \sqrt{(f_c \times [f_c - \sigma(z)])} \quad (6)$$

and for failure due to tension:

$$\nu_{ct}(z) = \sqrt{(f_c \times [f_c + \sigma(z)])}, \quad (7)$$

where:

$f_c$ compression strength of concrete and
$\sigma(z)$ normal stress at a point z due to the bending moment and axial force.

Coordinate z is the distance of a specific point to the compression edge of a section, as seen in Figure 2. Only Equation (6) will be used in this paper because only compressive failure is considered. It is apparent from Equation (6) that if a normal stress is equal to the strength, no further shear capacity exists in that point. This is clearly visible in Figure 2. The uniform distribution of stresses along a breadth of a section is assumed. The compressive shear capacity of a section is determined by the integration along the compressed part of the section. Therefore (Equation (8)):

$$V_{Rd} = \int \nu_{cc}(z) \times b_w \times dz, \quad (8)$$

where the integration limit ranges from zero to x, and x is the length of a compressed area.

A rectangular section under bending moment $M$ is shown in Figure 2, along with the strains $\varepsilon_c$, normal stresses $\sigma$ and allowable shear stresses $\nu_{cc}$. For strains $\varepsilon_c \geq 2‰$ (for normal strength concrete), normal stresses in concrete equal the compressive strength, i.e., $\sigma = f_c$. $F_S$ denotes the tensile force in tension steel. Three levels of curvature of a section are shown in Figure 2, from the smallest (left side) to the largest curvature (right side). It is evident from Figure 2 that increasing the ductility decreases the available shear area, and with it the shear strength.

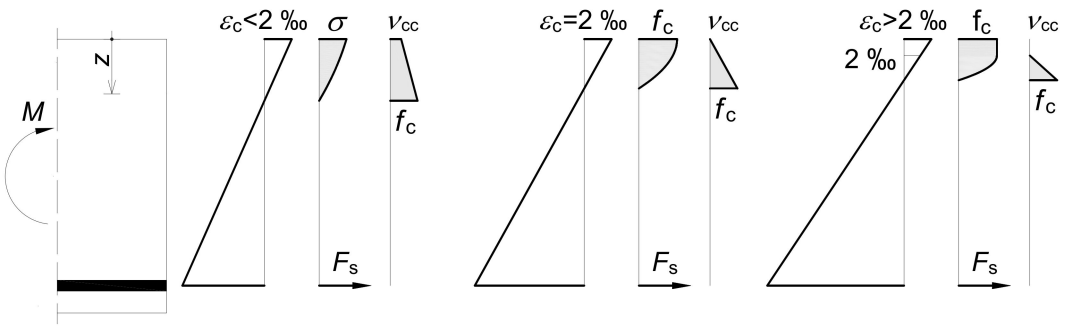


**Figure 2.** Normal and allowable shear stresses for different section curvatures.

Axial force also influences the curvature, but in addition it causes the reduction of lateral demand (it stabilizes a wall). Figure 3 shows a mechanism by which a reduction of lateral demand (or increase of lateral capacity) occurs, explained in detail in [13]. Axial force acts in the centre of the area of a cross section, but its reaction at the bottom of a wall acts on a smaller area due to cracking. Because of that, a deviation of force occurs, leading to a formation of a diagonal strut. In order for the system to stay in equilibrium, the moment developed by the axial force acting on a lever must be countered by a pair of lateral forces $V_n$. Such forces stabilize the system and reduce the part of the lateral force that causes stresses. Lateral force $V_n$ at the bottom of the wall will increase the demand for the storey below, but since a new axial force is introduced at every storey, the new reduction and the old increase are in equilibrium (if the level of axial force introduced at every level is the same). Therefore, only the axial force on one level should influence lateral resistance. Although the compressive length $x$ is different on each storey, the additional deviation of a force is considered to be very small and is disregarded in this paper. Axial tension force would reduce the compressive shear strength by a mechanism shown in Figure 3.

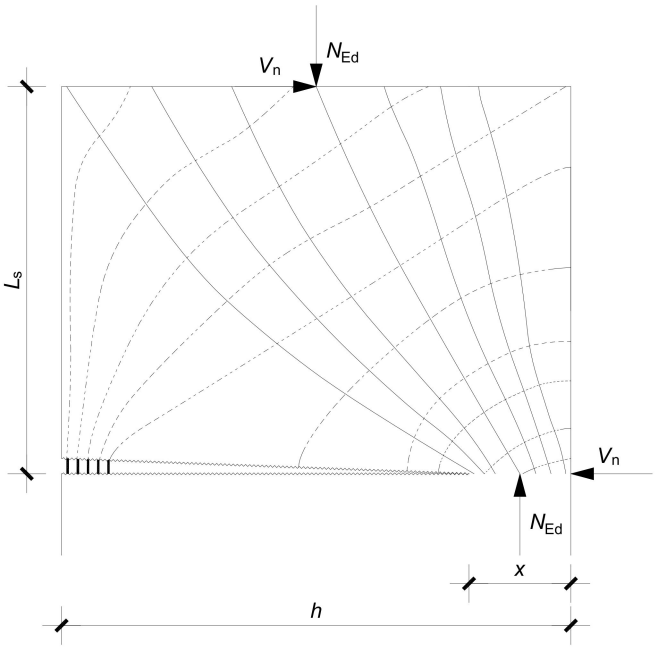


**Figure 3.** Reduction of a shear demand due to an arch mechanism.

According to Figure 3, considering the bending moment equilibrium, force $V_n$ can be calculated by (Equation (9)):

$$V_n = N_{Ed} \times (h - x)/(2 \times L_s). \quad (9)$$

Although the length of the compression zone changes with varying levels of ductility, the arch mechanism primarily depends on the ratio $h/L_s$.

Calculations are made considering the methods used in [11,13,33]. The method for determining characteristic points of the bending moment—curvature diagram is taken from [33] for rectangular and T-shaped sections and upgraded. In this paper, a procedure given in [33] is expanded by adding the influence of axial force (for further information please refer to the spreadsheet in Supplementary Materials which contains the calculation procedure for determining shear strength). The curvature is increased stepwise, and for each step the shear compressive strength is calculated. Methods from [33] are used only to determine the points of the bending moment—curvature diagram, since no shear strength was considered there. The method shown in [11] was used to determine the shear strength, but it was combined with the method used in [13] to consider the arch mechanism. Only rectangular cross sections are considered and compared with the values given in [6]. Average values from [6] are used, shown in Table 4. Some parameters from the original paper are omitted, such as the amount of confinement reinforcement, since its influence greatly depends on detailing, and no information is available regarding it.

**Table 4.** Average values of specimen parameters taken from [6].

| Parameter | $h$ [m] | $L_s/h$ | $h/b_w$ | $f_c$ [MPa] | $N/(A_c \cdot f_c)$ | $\rho_{tot}$ [%] |
|---|---|---|---|---|---|---|
| average value | 1.38 | 1.6 | 12.6 | 32.9 | 0.08 | 1.4 |

## 3. Results

The diagram of compressive shear strength reduction with respect to the increase of the curvature is shown in Figure 4. The values were obtained using the analytical procedure with parameters taken from Table 4. Because the ductility of a section taken from Table 4 is between 7 and 8, the ultimate compressive strain of concrete is taken as $\varepsilon_{cu2,c}$ = 5‰, simulating the confinement and achieving a ductility of 13. Reduction is a ratio of value obtained analytically and the value obtained using Equation (1).

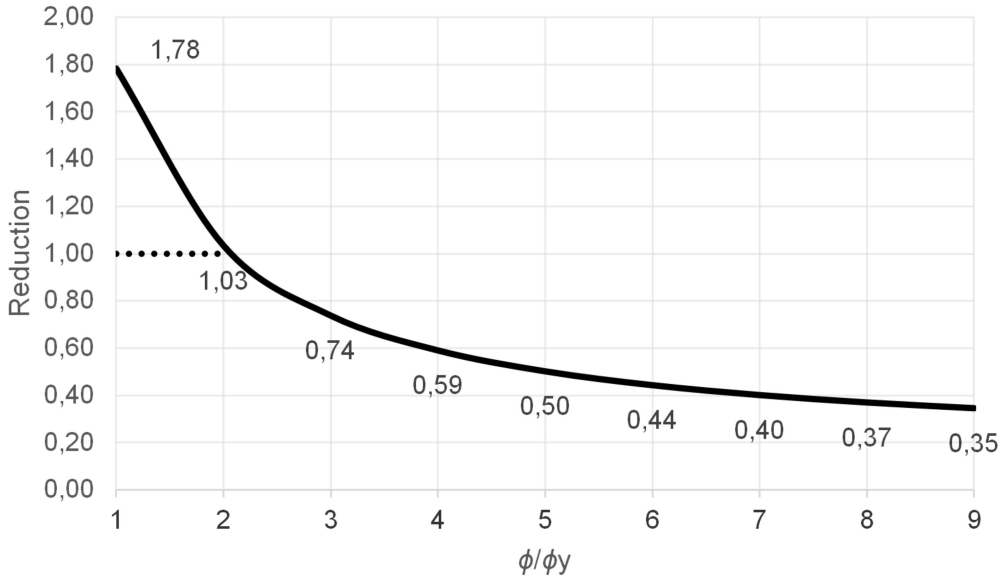


**Figure 4.** Reduction of compressive shear strength with the increase in ductility.

It can be seen from Figure 4 that the reduction of 0.4 proposed in [3] is achieved at curvature 7 (with parameters taken from Table 4) according to the analytical procedure. The reduction according to (2) (for the same parameters) is 0.53, which indicates that the analytical procedure is somewhat conservative.

According to Figure 4, for low curvatures the reduction is > 1. This does not mean that there is an increase in strength, but that crushing at such curvature may occur anywhere along the height of the wall (probably away from the bottom corner, which is usually heavily confined). At low curvatures, the dotted line represents the actual strength of an element, while the solid line considers only the bottom section.

In subsequent sections, different parameters are varied to determine their influence on the compressive shear strength and to develop an analytical expression which could be easy to understand and use.

### *3.1. Influence of Axial Force*

The influence of axial force at different levels of curvature on compressive shear strength is analytically determined and shown in Figure 5. Tensile force is not considered in this paper, since at critical sections of most walls compressive axial force occurs. Only the value of axial force is varied, while other parameters are kept constant, as shown in Table 4. According to previously determined levels of curvature at medium and high ductility levels, DCM is represented by a black line, while DCH is represented by a blue one.

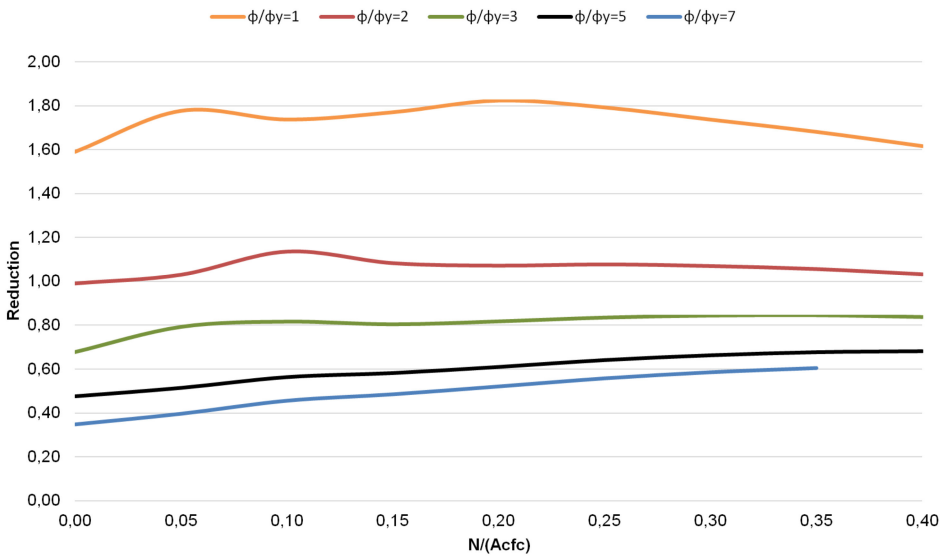


**Figure 5.** Influence of axial force on shear strength reduction.

Increasing the axial force decreases the available curvature ductility. For a section with parameters shown in Table 4, at an axial force level of $N/(A_c \times f_c) \geq 0.1$ the available ductility is less than 7 (if the ultimate compressive strain of concrete is 3.5‰). Confining can be used to increase the available compressive strain, and with it the available curvature ductility. Because of that, values of $N/(A_c \times f_c) \geq 0.1$ are also considered, simulating a possible confinement. The influence of confinement on compressive strength is also considered, as well as its influence on all the specific strains (ultimate strain and strain at peak stress) and strengths. The level of confinement considered in this paper is such that with the parameters from Table 4 at the force level $N/(A_c \times f_c) = 0.35$, the available ductility is 7. This value was chosen because, according to [3], the highest allowable level of axial force for DCH is $N/(A_c \times f_c) = 0.35$. This determines the maximum required confinement level. In order to consider only the influence of axial force, the confinement level (and with it the ultimate strain) is kept constant for all levels of axial force.

According to the analytical model used in this paper, the influence of axial force on shear strength changes with the curvature level. At a larger curvature, the increase of axial force increases the shear strength (lower reduction visible for the blue line at higher force levels in Figure 5). As mentioned before, for DCH only $N/(A_c \times f_c) \leq 0.35$ was considered, while for DCM, according to [3], the highest

allowable level of axial force is $N/(A_c \times f_c) = 0.4$. That is why for lower curvatures the values of reduction are presented up to $N/(A_c \times f_c) = 0.4$.

It is visible from Figure 5 that the increase in axial force causes an increase of shear strength at higher ductility levels, while at lower ductility levels this is not always the case. The increase of curvature causes an increase in the width of the horizontal crack. Compressive axial force partially closes this crack and allows for a larger area to transmit a shear force. In addition, the influence of the arch mechanism (Figure 3) becomes more important with the increase of axial force. Those are the reasons why axial force increases the strength. For a constant level of axial force, increasing the curvature would lead to a reduction of shear strength because the compressive length decreases. The arch mechanism is less dependent on the curvature, meaning that at higher curvatures it becomes more important.

### 3.2. Influence of the Amount of Longitudinal Reinforcement

The influence of the amount of longitudinal reinforcement at different levels of curvature on compressive shear strength is analytically determined and shown in Figure 6. Only the amount of longitudinal reinforcement is varied, while other parameters are kept constant at the values shown in Table 4. According to previously determined levels of curvature at medium and high ductility levels, DCM is represented by a black line, while DCH is represented by a blue one.

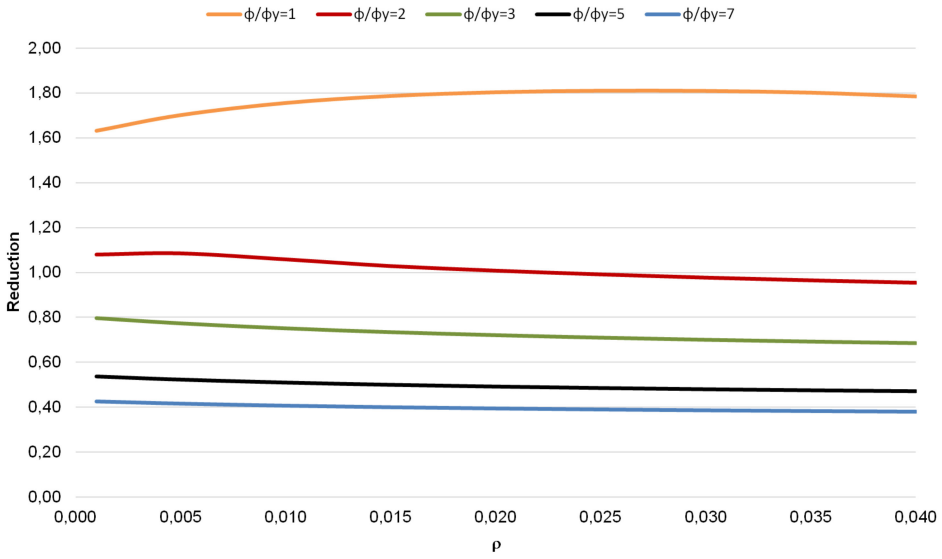


**Figure 6.** Influence of the amount of longitudinal reinforcement on shear strength reduction.

It is clear from Figure 6 that, according to the proposed analytical model, the influence of reinforcement on the shear strength at large curvatures is very small. This is the largest difference between the proposed model and the one given in [8], according to which the amount of reinforcement significantly influences the strength, retaining the same intensity regardless of the curvature. This is physically illogical, since at high curvatures a large amount of reinforcement has yielded.

At yield ($\phi/\phi_y = 1$), the increase of the amount of reinforcement is beneficial to the shear strength. A larger amount of reinforcement implies the greater force that it can carry and, because of that, the surface of the compressed concrete area (the area that transfers shear) needs to be larger. This increase has a limit because for a large amount of reinforcement, stress in concrete reaches strength. A further increase of steel increases the compressive area, but that area does not transfer shear. Increasing the curvature decreases the area that transfers shear. Two sections of the same geometry are shown in Figure 7. The cross section in the upper part of the figure has less reinforcement than the one in the lower part of the figure. It is clear from Figure 7 that for a low curvature shear strength increases, while the opposite is true for large curvatures.

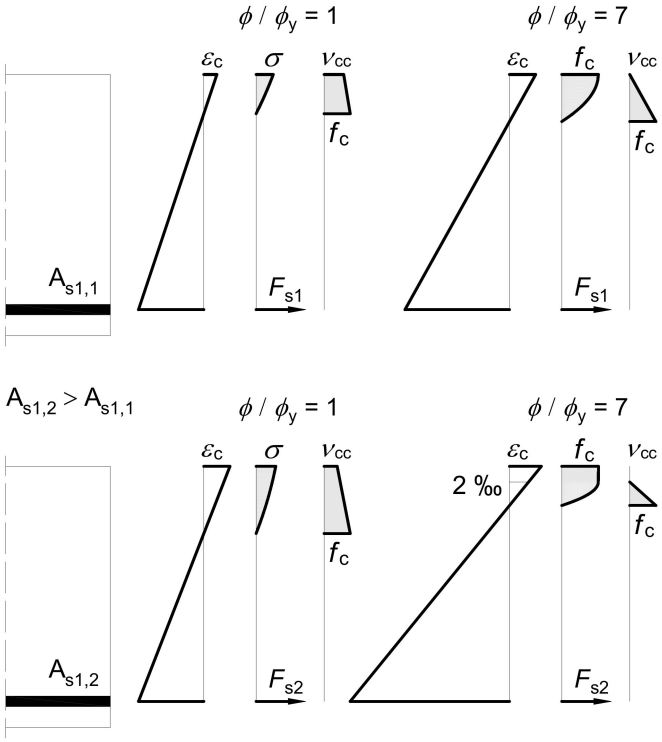


**Figure 7.** Influence of the amount of reinforcement and curvature on shear strength.

### *3.3. Influence of the Value of Ultimate Curvature*

In addition to the previously explained parameters, it is important to determine if the value of ultimate curvature (at which bending failure occurs) influences the shear strength. This could also be described as the influence of confinement. Code [3] requires a minimum level of ductility to be achieved, but larger values are allowed. Because of that, it is important to know the ultimate curvature (ductility), as well as the required one. Reductions $R$ at different levels of curvature for a specific ductility $\mu_\Phi$ are shown in Table 5. The first column consists of ductilities, the second column consists of reductions at a curvature $\phi/\phi_y = 2$, the third column consists of reductions at a curvature $\phi/\phi_y = 3$, and so on. Values ranging from $R_2$ to $R_{10}$ represent the shear strength reductions at curvatures from $\phi/\phi_y = 2$ to $\phi/\phi_y = 10$, respectively. In the final column, $R_u$ shows the value of reduction at the ultimate curvature. Reduction is defined as the ratio of shear strength calculated analytically and by Equation (1). The upper and lower values of ductility that were considered (8 and 16) are chosen arbitrarily to show the change at high ductilities. According to Equation (2), the influence of ductility on shear strength stops at 11, so 16 is taken to check the progression of shear strength after 11, while 8 is taken for comparison with lower values. All of the parameters are taken from Table 4. For the unconfined concrete, the available ductility is between 7 and 8. Higher ductilities are achieved by keeping all of the parameters constant, except for the ultimate strain of concrete (and compressive strength), thus simulating different levels of confinement. For a different amount of longitudinal reinforcement and different axial force, the values in the table would change. Row "13" corresponds to the values plotted in Figure 4.

What is important to notice is the fact that shear strength is not significantly influenced by ductility, and at a given curvature, it increases with the increase in ductility. Another important thing is to notice the change of values in the last column. At the level of ductility $\mu_\Phi = 11$ and higher, the reduction at the ultimate curvature becomes nearly constant. This should be compared with the provisions given in [8], since the value of shear strength given there is for the ultimate curvature. Although not exactly correct, this influence nearly becomes constant at the mentioned ductility.

When considering a specific section (a defined ductility), reduction changes with the increase in curvature, but this reduction becomes nearly constant for higher curvatures. This would correspond to the values in one row of Table 5.

**Table 5.** Shear strength reductions at different ductilities.

| $\mu_\Phi$ | $R_2$ | $R_3$ | $R_4$ | $R_5$ | $R_6$ | $R_7$ | $R_8$ | $R_9$ | $R_{10}$ | $R_u$ |
|---|---|---|---|---|---|---|---|---|---|---|
| 8 | 1.03 | 0.74 | 0.59 | 0.50 | 0.44 | 0.40 | 0.37 | - | - | 0.37 |
| 9 | 1.03 | 0.74 | 0.59 | 0.50 | 0.44 | 0.40 | 0.37 | 0.35 | - | 0.35 |
| 10 | 1.04 | 0.74 | 0.59 | 0.50 | 0.44 | 0.40 | 0.37 | 0.35 | 0.33 | 0.33 |
| 11 | 1.04 | 0.74 | 0.59 | 0.50 | 0.45 | 0.40 | 0.37 | 0.35 | 0.33 | 0.31 |
| 12 | 1.04 | 0.74 | 0.59 | 0.50 | 0.45 | 0.40 | 0.37 | 0.35 | 0.33 | 0.30 |
| 13 | 1.04 | 0.74 | 0.59 | 0.51 | 0.45 | 0.40 | 0.37 | 0.35 | 0.33 | 0.29 |
| 14 | 1.04 | 0.75 | 0.60 | 0.51 | 0.45 | 0.41 | 0.37 | 0.35 | 0.33 | 0.28 |
| 15 | 1.10 | 0.80 | 0.64 | 0.54 | 0.48 | 0.43 | 0.40 | 0.37 | 0.35 | 0.28 |
| 16 | 1.13 | 0.87 | 0.69 | 0.58 | 0.51 | 0.46 | 0.42 | 0.39 | 0.37 | 0.29 |

An important question arises from this analysis: should the reduction be made for a required curvature to which a design is made, or should it be made for the ultimate curvature that a section can sustain? In other words, if a curvature is reached, at which enough energy is dissipated, does the mode of failure matter? An analytical expression will be given later in this paper which considers the value of shear strength at the ultimate curvature. This is in accordance with the capacity design, but might be too strict a rule and should be cautiously considered.

It is worth mentioning that although the reduction remains nearly constant at higher curvatures, regardless of ductility, the actual value of shear strength increases with the increase of confinement (but so does the value calculated by Equation (1)).

### *3.4. Influence of the Reinforcement Arrangement*

In addition to the tension reinforcement visible in Figures 2 and 7, walls are usually reinforced with compression and web reinforcement. The assumed reinforcement arrangement is shown in Figure 8. An equal amount of reinforcement in tension and compression is assumed, as well as an equal reinforcement on both sides of the web.

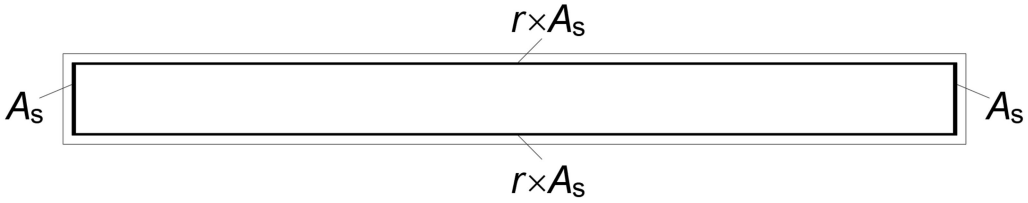


**Figure 8.** Cross section with the reinforcement arrangement.

The reinforcement shown in Figure 8 is vertical (perpendicular to the cross section) and uniformly distributed along a line. The reduction of shear strength at curvature $\phi/\phi_y = 7$ is shown in Table 6 for different reinforcement ratios $r$, while all other parameters were kept constant. Reduction is defined as a ratio of analytically defined shear strength and by Equation (1). It is visible from Table 6 that the arrangement of longitudinal reinforcement does not significantly influence the shear strength. It does influence, however, the ductility of a section (if the same total amount of reinforcement is achieved). Increasing the amount of web reinforcement (while keeping the total amount of reinforcement constant) leads to a decrease in ductility. Less edge reinforcement means that in order to satisfy equilibrium, a higher ultimate strain of steel is required. Theoretically, if a very low amount of edge reinforcement is present, a failure may occur at concrete strains lower than 3.5‰. This would mean that the influence of confinement is not utilized. Additionally, a lower amount of edge reinforcement means that a larger

part of the section is in tension. Since compression reinforcement increases ductility, this also leads to a reduction of ductility. The larger the ratio r, the lower the ductility. Stiffness, on the other hand, may be increased with the increase of the ratio r. Since the reinforcement closer to the edge of the section usually yields, it loses most of its stiffness. The reinforcement closer to the middle of the section is less likely to yield, so it might provide stiffness in the plastic part of the wall behaviour, causing a self-centring effect. Further analyses should be made to determine the stiffness degradation of walls. According to Equation (2), only the total amount of reinforcement influences the shear strength, which is in accordance with this analytical procedure.

**Table 6.** Shear strength reduction for different reinforcement ratios.

| $r$ | $R_7$ |
|---|---|
| 0.0 | 0.41 |
| 0.5 | 0.40 |
| 1.0 | 0.40 |
| 1.5 | 0.40 |
| 2.0 | 0.39 |

### *3.5. Adjusting the Analytic Procedure with the Existing Code*

When a standard design is made in accordance with [3], the required ultimate confined strain of concrete $\varepsilon_{cu2,c}$ is known, as well as the ultimate compression length $x_u$. The ultimate compression length can be determined either by using the equation 5.21 from code [3] or by an analytical procedure explained earlier in this paper. The ultimate strain of confined concrete can be determined by using the equation 3.1.9 from code [5] and considering the paragraph 5.4.3.4.2 (6) from code [3]. Using the basic geometry, a part of the section for which $\varepsilon_c < \varepsilon_{c2}$ can easily be found as $x' = \varepsilon_{c2}/\varepsilon_{cu2,c} \times x_u$. Shear is only transferred by an area $A_v = b_w \times x_u$, as can be seen on the far right of Figure 2. Normal stress increases parabolically from zero at neutral axis to compressive strength at the distance $x'$ from the neutral axis. Additionally, compressive axial force increases shear strength by an arch mechanism (as well as influencing the $x_u$). According to the analytical procedure, shear strength can be calculated by using the following Equation (10):

$$V_{Rd}{}^{an} = x' \times b_w \times \nu_{cc,av} + N_{Ed} \times (h - x)/(2 \times L_s), \quad (10)$$

where: $\nu_{cc,av}$ average value of allowable shear stress.

The explanation of $h$ and $L_s$ is visible in Figure 3. For concrete classes not greater than C50/60 (normal strength concrete), the parabolic part of the stress diagram is a second order parabola, and $\varepsilon_{c2} = 2‰$. The parabola can be replaced by a rectangle of the same area, in which case the height of that rectangle is $\sigma = 2/3 \times f_c$. Combining this with Equation (6), for concrete classes up to C50/60, Equation (11) can be derived:

$$\nu_{cc,av} = \sqrt{(f_c \times [f_c - 2/3 \times f_c])} = f_c/\sqrt{3}. \quad (11)$$

Equation (10) can, for concrete classes up to C50/60, be rewritten as (Equation (12)):

$$V_{Rd}{}^{an} = 2/\varepsilon_{cu2,c} \times x_u \times b_w \times f_c/\sqrt{3} + N_{Ed} \times (h - x)/(2 \times L_s). \quad (12)$$

In Equation (12) compressive force is positive.

Since all of the parameters used in (12) are known if the standard procedure given in [3] is followed, this equation does not complicate the calculation. Equation (12) is simple, easy to understand and based on well-known mechanisms. Only the most important mechanisms are considered, which enables the expression to be simple, but it makes it more conservative. The influence of the longitudinal reinforcement is "hidden" in the calculation of the ultimate compression length. The influence of the

confinement is considered with $\varepsilon_{cu2,c}$, and the influence of axial force is partly directly considered, and partly considered in the calculation of the ultimate compression length. The influence of ductility is considered with parameters $x_u$ and $\varepsilon_{cu2,c}$.

The shear strength determined by Equation (12) is the value at bending failure. A larger value of shear strength may be obtained if a smaller curvature is considered. As mentioned before, a detailed examination of the code is needed to determine which of the procedures should be used.

## 4. Discussion

As discussed before, the analytical procedure is somewhat conservative for some parameter values. There are a few reasons for this, one of them being the fact that strength was calculated in an additive manner (only adding mechanisms which are visible to the overall strength). There are probably more mechanisms that contribute to the strength which were not considered in this paper, such as the mechanical interlock of aggregates in part of the tension zone, which could lead to the transmission of a compression force. This might contribute to strength, but it is hard to predict and model. Moreover, a part of the tension zone is not cracked, which is disregarded in this paper (the standard assumption in concrete design is that the tensile strength is zero). Under dynamic loads, the compressive strength of concrete increases, which is also not considered in this paper. The tension strain limit of reinforcement lowers due to the dynamic nature of the load, which is not considered in this paper. It is also obvious that, at the level of reinforcement, the available shear strength is greater than at the locations where concrete is located. This is not considered in this paper, and a homogenous concrete material is assumed. Additionally, Rankine's theory is simple, and a better fitting of results might be possible with some other theory. According to Equation (2), shear strength becomes constant at $\mu_\theta{}^{pl} \geq 5$ ($\phi/\phi_y = 11$). Using the analytical procedure, a similar thing can be observed. Strength is not constant at high ductilities. Instead, the rate of reduction decreases significantly. Moreover, it does not always happen at the same curvature, but varies slightly. This phenomenon is also visible in Figure 4, where the curve becomes more flat with the increase in curvature.

From [6], it seems like the value of ultimate rotation $\phi_u$ used to calculate $\mu_\theta{}^{pl}$ (which is used in Equation (2)) is determined considering slip, which means that Equation (5) is not directly applicable. For a large slip at the ultimate load, the value of the actual curvature is smaller than the one obtained by Equation (5), because part of the rotation is due to slip (i.e., not all of the rotation comes from curvature). This explains why an analytical model would give seemingly lower strengths. Slip could be implemented in the analytical model, but it is not clear whether it should have been, since it does not significantly contribute to energy dissipation. Because Equation (2) was derived for $1.0 \leq L_s/h \leq 2.5$, it is questionable if $T_1 \geq T_C$, assumed in Equation (5), is correct. Additionally, only the amount of transverse reinforcement from the experimental data is known, and not its distribution. Since the empirical expression is derived from a large number of specimens with different geometries, it is unlikely that the distribution of reinforcement is similar in all of the specimens. Therefore, the ultimate concrete strain of the specimens is unknown. Because of the mentioned problems, a direct comparison of analytical and empirical procedures was avoided, as it would not give meaningful results.

More important than the difference in the values of reduction, however, is the fact that a reduction exists for DCM (roughly at $\phi/\phi_y = 5$, as previously noted). According to the analytical procedure, this reduction is 0.5, and according to (2) it is 0.57 (using the average parameter values from Table 4). Both of these reductions are large and should be taken into account, which is currently not done for new buildings. The reduction determined from experiments for DCM can be found in [6], where the median value of reduction is 0.515, which is very close to the two values mentioned earlier. Since most buildings are designed, in practice, with DCM, and since this failure mode is brittle, this seems like an important issue.

The empirical equation was derived by fitting to the median value of experimental data. While this might be appropriate for the evaluation of the behaviour of existing buildings, it might not be acceptable for the design of new ones. A lower value of strength should be adopted for achieving reliable design.

Additionally, the influence of reinforcement seems to have no upper limit in Equation (2). No mechanism explaining this phenomenon could be derived. This seems illogical, since at large curvatures most of the longitudinal reinforcement has yielded.

## 5. Conclusions

From the parametric theoretical analysis conducted in this paper, the following can be concluded:

- Axial force significantly influences compressive shear strength, which is increased by compressive force.
- The longitudinal reinforcement ratio slightly influences compressive shear strength at high curvatures. There is an upper limit to the influence of the reinforcement.
- The ultimate curvature of a section has no influence on compressive shear strength at a specific curvature, but does influence compressive shear strength at an ultimate curvature.
- The reinforcement arrangement inside a section does not influence compressive shear strength at a specific curvature, but does influence the ductility and stiffness of the element.
- The reduction of compressive shear strength is recommended for medium-ductility structures.
- The reduction of compressive shear strength is not correlated with the dynamic nature of the response.

Further research may be aimed at implementing a more advanced analysis, considering some of the parameters ignored in this paper. It also needs to be thoroughly compared with the experimental data.

Designers following the current code provisions should consider a more detailed analysis, as compressive shear strength may be critical to the behaviour of a structure.

**Supplementary Materials:** The following are available online at http://www.mdpi.com/2071-1050/12/11/4434/s1, Spreadsheet S1: manuscript-supplementary.xls.

**Author Contributions:** Conceptualization, T.K. and D.L.; data curation, I.H.; formal analysis, T.K. and T.R.; investigation, T.K. and T.R.; methodology, T.K., T.R. and I.H.; project administration, D.L.; resources, D.L.; software, T.K., T.R. and I.H.; supervision, D.L.; validation, T.R. and I.H.; visualization, T.K. and I.H.; writing—original draft, T.K. and T.R.; writing—review & editing, D.L. and I.H. All authors have read and agreed to the published version of the manuscript.

**Funding:** This research received no external funding.

**Conflicts of Interest:** The authors declare no conflicts of interest.

## References

1. Paulay, T.; Priestley, M.J.N. *Seismic Design of Reinforced Concrete and Masonry Buildings*, 1st ed.; John Wiley & Sons, Inc.: New York, NY, USA, 1992; p. 744.
2. Penelis, G.G.; Penelis, G.G. *Concrete Buildings in Seismic Regions*, 1st ed.; Taylor & Francis: Boca Raton, FL, USA, 2014; p. 826.
3. *Eurocode 8: Design of Structures for Earthquake Resistance—Part 1: General Rules, Seismic Actions and Rules for Buildings*; EN 1998-1; CEN: Brussels, Belgium, 2004.
4. *Eurocode 8: Design of Structures for Earthquake Resistance—Part 3: Assessment and Retrofitting of Buildings*; EN 1998-3; CEN: Brussels, Belgium, 2004.
5. *Eurocode 2: Design of Concrete Structures—Part 1-1: General Rules and Rules for Buildings*; EN 1992-1-1; CEN: Brussels, Belgium, 2004.
6. Grammatikou, S.; Biskinis, D.E.; Fardis, M.N. Strength, deformation capacity and failure modes of RC walls under cyclic loading. *Bull. Earthq. Eng.* **2015**, *11*, 3277–3300. [CrossRef]
7. Biskinis, D.E.; Roupakias, G.K.; Fardis, M.N. Degradation of Shear Strength of Reinforced Concrete Members with Inelastic Cyclic Displacements. *ACI Struct. J.* **2004**, *101*, 773–783.
8. Biskinis, D.E.; Fardis, M.N. Cyclic shear resistance model for Eurocode 8 consistent with the second-generation Eurocode 2. *Bull. Earthq. Eng.* **2020**, *18*, 2891–2915. [CrossRef]
9. *Designers Guide to EN 1998-1 and EN 1998-5*; Gulvanessian, H. (Ed.) Thomas Telford: London, UK, 2005; p. 279.

10. *Model Code 2010*; fib Bulletin 56; FIB: Lausanne, Switzerland, 2010; Volume 2.
11. Park, H.G.; Yu, E.J.; Choi, K.K. Shear-strength degradation model for RC columns subjected to cyclic loading. *Eng. Struct.* **2012**, *34*, 187–197. [CrossRef]
12. Sezen, H.; Moehle, J.P. Shear Strength Model for Lightly Reinforced Concrete Columns. *J. Struct. Eng.* **2004**, *130*, 1692–1703. [CrossRef]
13. Priestley, M.J.N.; Verma, R.; Xiao, Y. Seismic shear strength of reinforced concrete columns. *J. Struct. Eng.* **1994**, *120*, 2310–2329. [CrossRef]
14. Ang, B.G.; Priestley, M.J.N.; Paulay, T. Seismic Shear Strength of Circular Reinforced Concrete Columns. *Struct. J.* **1989**, *86*, 45–59.
15. Li, Y.; Hwang, S.J. Prediction of Lateral Load Displacement Curves for Reinforced Concrete Short Columns Failed in Shear. *J. Struct. Eng.* **2017**, *143*, 04016164. [CrossRef]
16. Pan, Z.; Li, B. Truss-Arch Model for Shear Strength of Shear-Critical Reinforced Concrete Columns. *J. Struct. Eng.* **2013**, *139*, 548–560. [CrossRef]
17. Fu, L.; Nakamura, H.; Furuhashi, H.; Yamamoto, Y.; Miura, T. Mechanism of shear strength degradation of a reinforced concrete column subjected to cyclic loading. *Struct. Concr.* **2017**, *18*, 177–188. [CrossRef]
18. Hua, J.; Eberhard, M.O.; Lowes, L.N.; Gu, X. Modes, Mechanisms, and Likelihood of Seismic Shear Failure in Rectangular Reinforced Concrete Columns. *J. Struct. Eng.* **2019**, *145*, 04019096. [CrossRef]
19. Terzioglu, T.; Orakcal, K.; Massone, L.M. Cyclic lateral load behavior of squat reinforced concrete walls. *Eng. Struct.* **2018**, *160*, 147–160. [CrossRef]
20. Ni, X.; Cao, S.; Liang, S.; Li, Y.; Liu, Y. High-strength bar reinforced concrete walls: Cyclic loading test and strength prediction. *Eng. Struct.* **2019**, *198*, 109508. [CrossRef]
21. Chen, X.L.; Fu, J.P.; Hao, X.; Yang, H.; Zhang, D.Y. Seismic behavior of reinforced concrete squat walls with high strength reinforcements: An experimental study. *Struct. Concr.* **2019**, *20*, 911–931. [CrossRef]
22. Baek, J.W.; Park, H.G.; Shin, H.M.; Yim, S.J. Cyclic Loading Test for Reinforced Concrete Walls (Aspect Ratio 2.0) with Grade 550 MPa (80 ksi) Shear Reinforcing Bars. *ACI Struct. J.* **2017**, *114*, 673–686. [CrossRef]
23. Baek, J.W.; Park, H.G.; Lee, J.H.; Bang, C.J. Cyclic Loading Test for Walls of Aspect Ratio 1.0 and 0.5 with Grade 550 MPa (80 ksi) Shear Reinforcing Bars. *ACI Struct. J.* **2017**, *114*, 969–982. [CrossRef]
24. Salonikios, T.N. Analytical Prediction of the Inelastic Response of RC Walls with Low Aspect Ratio. *J. Struct. Eng.* **2007**, *133*, 844–854. [CrossRef]
25. Rutenberg, A. Seismic shear forces on RC walls: Review and bibliography. *Bull. Earthq. Eng.* **2013**, *11*, 1727–1751. [CrossRef]
26. Rejec, K.; Isaković, T.; Fischinger, M. Seismic shear force magnification in RC cantilever structural walls, designed according to Eurocode 8. *Bull. Earthq. Eng.* **2012**, *10*, 567–586. [CrossRef]
27. Yathon, J.S. Seismic Shear Demand in Reinforced Concrete Cantilever Walls. Ph.D. Thesis, The University of British Columbia, Vancouver, BC, Canada, April 2011.
28. Rivera, J.P.; Whittaker, A.S. Damage and Peak Shear Strength of Low-Aspect-Ratio Reinforced Concrete Shear Walls. *J. Struct. Eng.* **2019**, *145*, 04019141. [CrossRef]
29. *Building Code Requirements for Structural Concrete*; ACI 318-14; ACI: Farmington Hills, MI, USA, 2011.
30. *Standard Specifications for Concrete Structures "Design"*; JSCE No. 15; JSCE: Tokyo, Japan, 2007.
31. *Concrete Structures Standard—Part 1—The Design of Concrete Structures*; NZS 3101-1; SNZ: Wellington, New Zealand, 2006.
32. Chen, W.F. *Plasticity in Reinforced Concrete*, 1st ed.; McGraw-Hill: New York, NY, USA, 1982; p. 474.
33. Kišiček, T.; Sorić, Z. Bending moment-curvature diagram for reinforced-concrete girders. *Građevinar* **2003**, *55*, 207–215.